Radiation Damage of Standard and Oxygenated Silicon Diodes by 16 and 27 MeV Protons

D. Bisello[1,2], J. Wyss[3,4], A. Candelori[1,2], A. Kaminsky[2], D. Pantano[1,2]

[1]Istituto Nazionale di Fisica Nucleare, Sezione di Padova, via Marzolo 8, I-35131 Padova, Italy

[2]Dipartimento di Fisica, Università di Padova, via Marzolo 8, I-35131 Padova, Italy

[3]Facoltà di Ingegneria, Università di Cassino, via Di Biasio 43, I-03043 Cassino (FR), Italy

[4]Istituto Nazionale di Fisica Nucleare, Sezione di Pisa, via Livornese 1291, I-56010 Pisa, Italy

Abstract

The effects of irradiation by 16 MeV and 27 MeV protons on standard and oxygenated silicon diodes, processed by different technologies, have been investigated. The acceptor creation rate β, after type inversion can be lower for standard diodes than for state of the art oxygenated devices, suggesting that the role of oxygen is more complex than expected and must be folded with the technology of the fabrication process. In addition we show the inaccuracy of the β normalization by the non-ionizing energy loss (NIEL) factor not only for oxygenated diodes but also for standard non-oxygenated devices.

I. Introduction

It is well known that under irradiation the presence in silicon of high oxygen concentrations up to $[O] \approx 2 \cdot 10^{17}$ O/cm^3 does not affect the volumetric leakage current increase rate α, which depends on energy and type of radiation, in agreement with the NIEL scaling model [1-6]. On one hand, the acceptor creation rate (β) after neutron irradiation is not significantly affected by the oxygen concentration [1-4]; on the other hand, β and consequently the depletion voltage (Vdep) is dramatically reduced, and by the same amount, in oxygenated diodes irradiated by 24 GeV protons and 192 MeV pions [2-5] whereas this effect is smaller for 27 MeV protons [7]. Oxygen-based models have been proposed to explain the capability of oxygen to suppress the formation of V_2O centers considered to be responsible for changes in Vdep after irradiation [8].

The β behavior under charged hadron irradiation shows that the non-ionizing energy loss (NIEL) factors are not sufficient to normalize the acceptor creation rate for oxygenated devices [3,4]. Moreover our group has recently reported that β cannot be scaled by NIEL factors even for standard silicon devices after low energy proton irradiation [9]. In addition, other studies summarized in [10] have shown that β values for standard silicon diodes fabricated with different process can vary significantly, thus confirming the limits of the NIEL hypothesis, whereas oxygenated diodes are less sensitive to the fabrication process and their βs are systematically lower than those of the standard diodes.

In this work we report further on the evidence of the role of processing for what concerns the acceptor creation rate for standard and oxygenated diodes, showing that lower β values can be found for standard devices than for state of the art oxygenated diodes. In the light of this evidence, oxygen-based models appear to be too restrictive without taking into account other impurities and/or processing step effects, which affect the radiation induced acceptor creation rate.

II. Devices, Experimental Conditions and Electrical Measurements

The devices tested are state of the art silicon diodes fabricated by ITE [11] and ST Microelectronics [12]. The bulk of all the diodes was initially n-type with resistivity of 1.3–3 kΩ·cm. The active area is surrounded by a n^+ guard-ring. The ITE devices were provided to us by the ROSE collaboration [13]. They were processed in both standard ($[O]_{standard} < 4 \cdot 10^{16}$cm^{-3}) and oxygenated ($[O]_{oxygenated} > 10^{17}$cm^{-3}) Si substrates. The standard diodes were obtained from wafers produced by Polovodice (PV) [14]. The oxygenated devices (JO) were processed on wafers by ITME [15]: oxygen was introduced by a jet of gas during the refining process. The ST Microelectronics diodes (ST) were processed on wafers with standard oxygen concentrations from Waker [16].

The geometrical dimensions and the oxygen and carbon concentrations of the PV and JO diodes, measured by SIMS at EVANS [17], are summarized in Table 1 along with data provided to us by ST. A new SIMS analysis of the carbon and oxygen content of the ST diodes is underway.

Table 1
Typical diode characteristics.

	PL	JO	ST
Area (cm^2)	0.25	0.25	0.25
Thickness (μm)	285	307	305
[O] (cm^3)	<4· 10^{16}	2.1-2.3· 10^{17}	<4· 10^{16}
[C] (cm^3)	9· 10^{15}	1· 10^{16}	≤9· 10^{15}

Irradiations were performed in two periods at the SIRAD irradiation facility of the Tandem accelerator at the INFN Laboratori Nazionali di Legnaro (Padova, Italy) [18]. In the first (second) period the standard PV and the oxygenated JO diodes (the standard PV and ST devices) were irradiated; i.e. the PV diodes were considered as reference devices.

During each period all the diodes were simultaneously irradiated without bias in cumulative steps at room temperature. At least two diodes of the same type were irradiated in the same experimental conditions: a proton (p) beam of 27 MeV was rastered with a uniformity of a few percent across the sample holder where the diodes were arranged in two rows. The diodes of one row received directly the 27 MeV protons; the other diodes were placed immediately behind a 2.45 mm thick silica strip that degrades the proton energy down to 15.7 MeV (FWHM≈0.7 MeV). This energy is still large enough to guarantee a uniform energy loss along the proton path in a ≈300 μm thick silicon diode. The fraction of protons scattered by the silica strip away from the diodes in the low energy row is calculated to be negligible. The energy degradation and the scattering estimate due to the silica strip were evaluated with SRIM [19].

The proton flux was measured on-line by a square 3-by-3 battery of independent small Faraday cups positioned 10 cm behind the target plane. A fluence of 10^{13} p/cm^2 is typically accumulated in 15 minutes; the initial fluence ($\Phi > 3\cdot10^{13}$ p/cm^2) was chosen so that the diodes were type inverted.

After each irradiation step the devices were thermally annealed at 80°C for 4 minutes in order to complete the beneficial annealing for the depletion voltage Vdep [1-5]. After annealing the devices were characterized by current-voltage (I-V) and 1 kHz, 10 kHz and 100 kHz capacitance-voltage (C-V) measurements by a HP4142 B modular DC source monitor and a HP4284A LCR meter, respectively. During the electrical characterization the reverse bias voltage (Vbias) was applied to the backside contact, while the n^+ guard-ring was grounded.

III. Experimental Results: PV and JO diodes

The depletion voltage used in reporting the following results is defined as the intersection point of the two different slopes on a log-log scale of the 10 kHz C-V curve, as shown in Figure 1 for a standard PV diode after receiving 27 MeV protons for a cumulative delivered fluence of $9\cdot10^{13}$ p/cm^2. The C-V curves of the oxygenated JO devices show the same shape of the PV diodes.

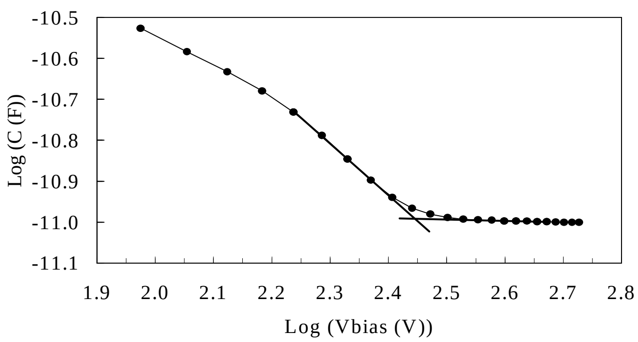

Figure 1. C-V measurement at 10 kHz for a PV diode after the cumulative delivered 27 MeV proton fluence of $9\cdot10^{13}$ p/cm^2.

The effective doping concentration Neff has been calculated by:

$$\text{Neff}=\frac{2\varepsilon}{qW^2}\,\text{Vdep} \qquad (1)$$

where W is the thickness of the diode, ε is the absolute Si dielectric constant and q is the electron charge.

The Neff data versus the cumulative delivered fluence Φ for PV and JO diodes, irradiated by 16 MeV and 27 MeV protons, are shown in Figure 2. As expected, Neff increases linearly by increasing Φ, being the diode substrate type inverted just before the first irradiation step. The acceptor creation rate β, that is the slope of the Neff(Φ) curve after substrate inversion, is lower for oxygenated diodes at both proton energies. Moreover β depends on the proton energy in a sizeable way and is lower for 16 MeV protons, whereas the NIEL is expected to increase by decreasing the proton energy [20].

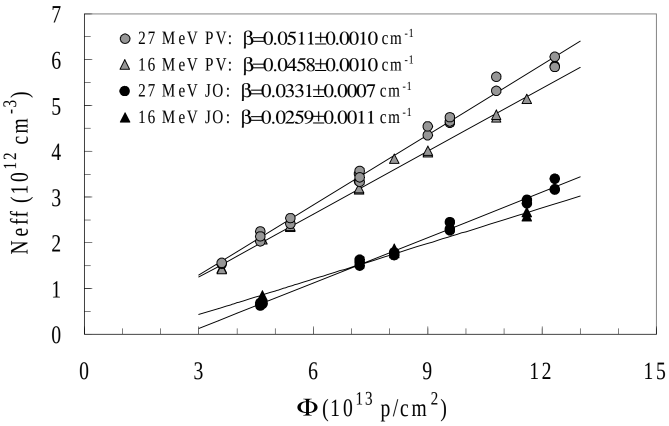

Figure 2. Neff for PV (dashed symbols) and JO (close symbols) diodes as a function of the cumulative delivered fluence for 27 MeV (circles) and 16 MeV (triangles) protons. The solid lines are linear fits of the experimental data; the β parameters are also reported.

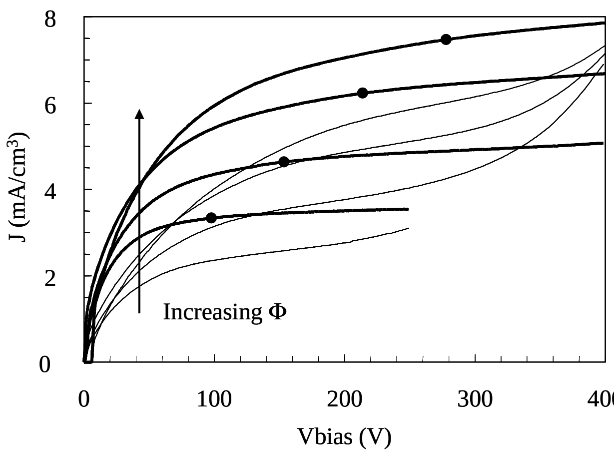

Figure 3. Diode (solid thick line) and guard-ring (solid thin line) current densities normalized to 20°C for PV devices irradiated by 27 MeV protons at $\Phi_1 = 3.6\cdot10^{13}$ p/cm^2, $\Phi_2 = 5.4\cdot10^{13}$ p/cm^2, $\Phi_3 = 7.2\cdot10^{13}$ p/cm^2 and $\Phi_4 = 9\cdot10^{13}$ p/cm^2. The circles on the four diode curves mark the diode current density at full depletion.

The current densities J=I/Vol, where I and Vol are the currents and the volume of the diode, respectively, have been normalized to 20°C by considering the temperature dependence [21] $J(T)=AT^2\cdot\exp(-E/2k_BT)$, where A is a constant, T is the absolute temperature, k_B is the Boltzmann constant and E=1.24 eV.

The diode (J_D) and guard-ring (J_{GR}) current densities normalized to 20°C are shown in Figure 3 for a PV diode as a function of Vbias, at each cumulative delivered fluence after

27 MeV proton irradiation. As expected, J_D monotonically increases by increasing Vbias, Vdep is within the low slope region of the J-V curve and J_{GR} is lower than J_D even beyond full depletion. Similar results were obtained for the JO diodes.

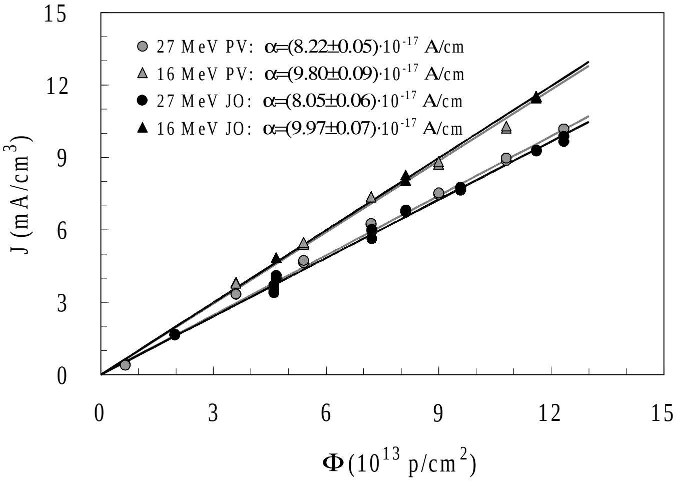

Figure 4. J_D normalized to 20°C at full depletion for PV (dashed symbols) and JO (close symbols) diodes as a function of the 27 MeV (circles) and 16 MeV (triangles) cumulative delivered proton fluence. The solid lines are linear fits of the experimental data; the α parameters are also reported.

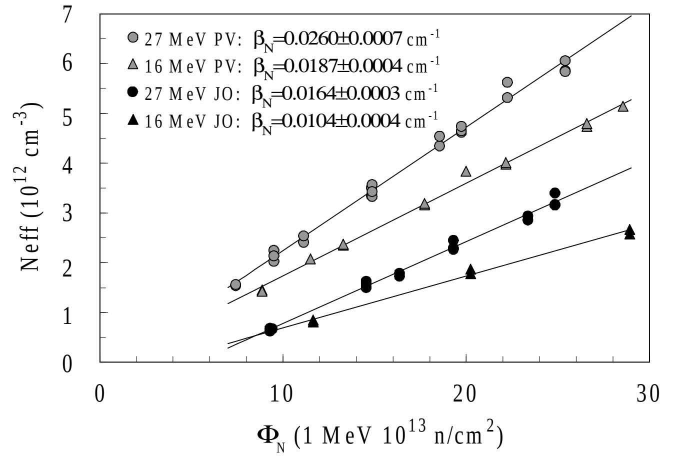

Figure 5. Neff as a function of 1 MeV neutron equivalent fluence for PV (dashed symbols) and JO (close symbols) diodes irradiated by 27 MeV (circles) and 16 MeV (triangles) protons. The solid lines are linear fits of the experimental data; the β_N parameters are also reported.

The J_D data measured at Vdep and normalized to 20°C as a function of Φ are shown in Figure 4 for PV and JO diodes. As expected, J_D is proportional to the cumulative delivered fluence; i.e. $J_D=\alpha\Phi$. The volumetric leakage current increase rate $\alpha=\alpha(X,E_X)$ depends on the radiation type X and on its energy E_X but it does not depend on the device oxygen concentration. The α parameter is higher for 16 MeV protons in agreement with the NIEL scaling hypotesis:

$$\alpha(X,E_X)/\alpha(Y,E_Y)=k(X,E_X)/k(Y,E_Y) \qquad (2)$$

where k is the hardness factor [21] of radiation X at energy E_X. By using the experimentally determined values of α at a standard temperature of 20°C, shown in Figure 4, the 27 MeV and 16 MeV cumulative delivered proton fluences have been normalized to the 1 MeV neutron equivalent fluence (Φ_N) by:

$$\Phi_N=\Phi\ \frac{\alpha(\text{proton};E)}{\alpha(\text{neutron};1\text{MeV})} \qquad (3)$$

where α(neutron,1 MeV)=$4\cdot10^{-17}$ A/cm [6].

After normalization, the Neff data for 16 MeV and 27 MeV protons, as a function of Φ_N (see Figure 5), do not overlap for both standard and oxygenated diodes, confirming that the β parameter does not scale by the NIEL factor not only for oxygenated but also for standard devices, at least for low energy protons. The slope of the Neff(Φ_N) line, that is the β_N parameter, is smaller for the JO diodes, and for a fixed device type it is lower for devices irradiated by 16 MeV protons. This suggests that there is a similar energy dependence for a given oxygen concentration. In particular the energy dependence of β_N for PV diodes indicates that the suppression of acceptor creation occurs at low proton energy even with very small oxygen concentrations.

IV. Experimental Results: ST Diodes

The ST diodes show a somewhat peculiar behaviour. At high cumulative delivered fluences (>$6\cdot10^{13}$ p/cm^2) the C-V curves at the standard 10 kHz frequency used to determine Vdep present an anomalous peak structure completely absent in the standard PV and JO diodes (see Figure 6). The structure grows with fluence and is more pronounced for C-V measurements at 1 kHz, while it is practically absent at 100 kHz. This structure may introduce a systematic error in the Vdep determination at the highest fluences, which nevertheless is expected to be small in our analysis because the linear fit of the C-V curve in the low slope region is well outside of the peak region, as shown in Figure 6.

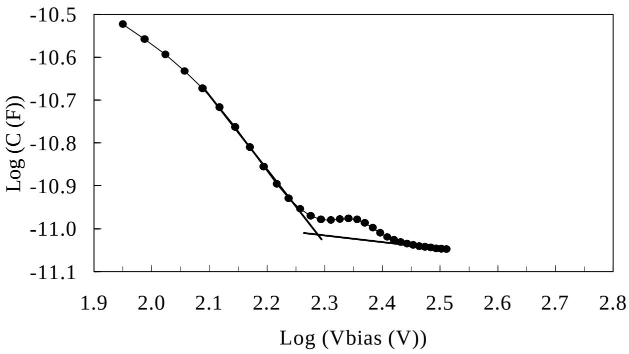

Figure 6: C-V measurement at 10 kHz for a ST diode after the cumulative delivered 27 MeV proton fluence of $9\cdot10^{13}$ p/cm^2.

The Neff(Φ) curves determined by the C-V measurements for the ST diodes are shown in Figure 7: the β parameter is lower for devices irradiated by 16 MeV protons, as already observed with the PV and JO diodes. The standard ST Neff(Φ) curves are surprisingly close to the data shown in Figure 2 for the oxygenated JO devices. Even though the two ST diodes irradiated by 27 MeV protons show a small data dispersion, β is lower for standard ST diode than for state of the art oxygenated devices. This suggests that other impurities and/or effects in processing steps affect the radiation hardening of the final device in order to obtain low β values.

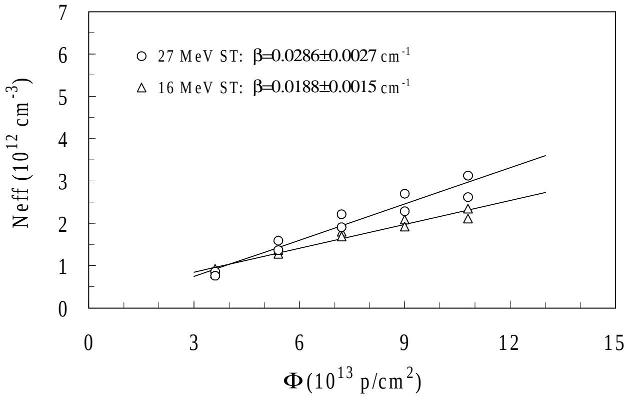

Figure 7: Neff for ST diodes as a function of the cumulative delivered fluence for 27 MeV (circles) and 16 MeV (triangles) protons. The solid lines are linear fits of the experimental data; the β parameters are also reported.

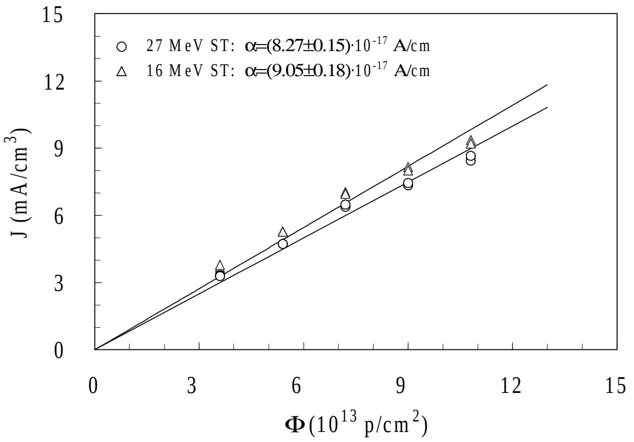

Figure 8. J_D normalized to 20°C at full depletion for ST diodes as a function of the 27 MeV (circles) and 16 MeV (triangles) cumulative delivered proton fluence. The solid lines are linear fits of the experimental data; the α parameters are also reported.

The correlation J_D at Vdep of the ST diodes as a function of Φ, shown in Figure 8, is not as good as that obtained for PV and JO diodes (see Figure 4): the experimental data seem to deviate from linearity at the highest fluences. In addition the ST α values disagree somewhat with the PV and JO data, even if the ST α is again higher for the 16 MeV proton irradiated diodes, as in Figure 4. The peculiarities of the ST α values are due to the anomalous behavior of the diode and guard-ring currents (see Figure 9), which affects the J_D measurement at Vdep, especially for high fluences. We recall that J_{GR} is lower than J_D in PV and JO diodes up to Vbias values significantly higher than Vdep, and J_D monotonically increases by increasing Vbias (see Figure 4). On the contrary, the ST J_{GR} (Figure 9) starts to increase quickly at values of Vbias the nearer to Vdep the higher the received fluence, reaching 50 mA/cm^3 at 400 V. Correspondingly the diode current density J_D decreases. These anomalous behaviors indicate that our measurements do not well estimate J_D at Vdep by an amount which increases with the fluence. Using the face values of Vdep obtained with the standard procedures used for the PV and JO diodes, we obtain the results plotted in Figure 8.

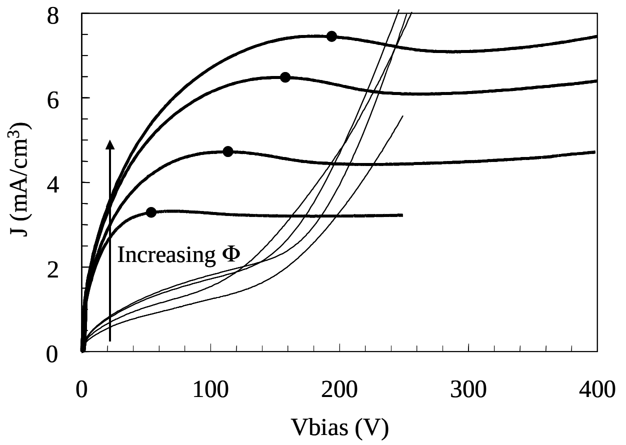

Figure 9. Diode (solid thick line) and guard-ring (solid thin line) current densities normalized to 20°C for ST devices irradiated by 27 MeV protons at Φ_1=3.6·10^{13} p/cm^2, Φ_2=5.4·10^{13} p/cm^2, Φ_3=7.2·10^{13} p/cm^2 and Φ_4=9·10^{13} p/cm^2. The solid circles on the four diode curves mark the diode current density at full depletion.

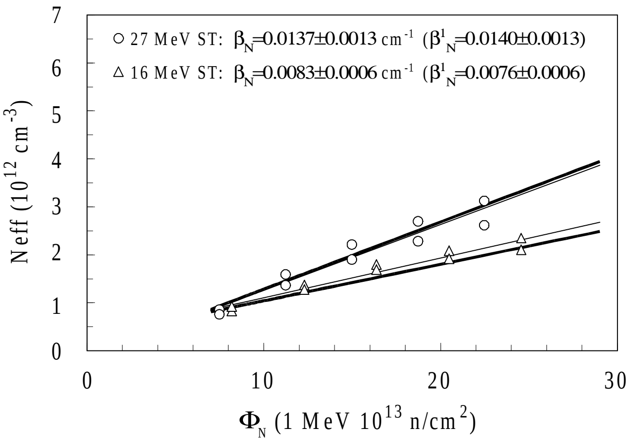

Figure 10. Neff for ST diodes as a function of the 1 MeV neutron equivalent fluence. Devices were irradiated by 27 MeV (circles) and 16 MeV (triangles) protons. The thin solid lines are linear fits of the experimental data; the β_N parameters are also reported. The thick solid lines are linear fits, whose β^1_N parameters are also reported, obtained by normalizing the 27 MeV (16 MeV) proton fluence to 1 MeV neutron by considering the average value of all the 27 MeV (16 MeV) PV and JO α values.

The values of β_N obtained for the ST diodes by considering the α values of Figure 6 for normalization of the proton fluence to the 1 MeV neutron equivalent value are shown in Figure 10. In the same figure we also report the fits which are obtained if the proton fluence normalization is performed by considering the average α value of the PV and JO diodes irradiated by protons with the corresponding energy. The slopes β^1_N of these fits are compatible with the above β_N within the fitting parameter error. In spite of the reported difficulties in determining Vdep and J_D at full depletion, the data of the ST diodes present qualitatively the same energy dependence of β_N shown for the standard PV and oxygenated JO diodes. However standard ST diodes have values of β_N that are significantly small, even smaller than those of the oxygenated JO devices.

V. Conclusions

We have shown that, in silicon diodes irradiated by 27 MeV and 16 MeV protons, the acceptor creation rate β, after type inversion, is sensitive to the energy of the impinging particles also for standard (non-oxygenated) material. This effect is amplified when the delivered fluences are normalized to the 1 MeV neutron equivalent values in disagreement with the currently accepted NIEL hypothesis. The β parameter decreases in a significant way when the proton energy is lowered by 27 MeV to 16 MeV. It is worth noting that on the contrary the leakage current damage constant α is independent of the oxygen content and increases by lowering the proton energy, in good quantitative agreement with NIEL expectations.

When processed the same way, oxygenated diodes show a lower acceptor creation rate than the standard ones, the effect being lower of a factor 2-3 at these proton energies than for 24 GeV protons.

However standard diodes fabricated from silicon wafers of similar characteristics (in particular resistivity) with a different process show an acceptor creation rate which can be lower than that of highly oxygenated diodes.

A further comparison of the behavior of standard and oxygenated ST diodes is underway. The data of the ST diodes presented here indicate, at least qualitatively, that the role of oxygen in affecting the acceptor creation rate is not yet completely understood. High oxygen concentrations play an important role in improving the hardening of the starting material, but the effects of other impurities and/or processing steps can be quite important in changing the acceptor creation rate β and in assessing the radiation hardness of silicon detector. Therefore these effects must be systematically investigated in order to understand the behavior of the low β standard silicon devices.

VI. References

[1] A. Ruzin, G. Casse, M. Glaser and F. Lemeilleur, "Studies of radiation hardness of oxygen enriched silicon detectors", Nucl. Instr. and Meth., vol.A 426, pp.94-98, 1999.

[2] A. Ruzin, "Recent results from the RD-48 (ROSE) Collaboration", Nucl. Instr. and Meth., vol.A 447, pp.116-125, 2000.

[3] A. Ruzin, G. Casse, M. Glaser, F. Lemeilleur, R. Talamonti, S. Watts and A. Zanet, "Radiation hardness of silicon detectors manufactured on epitaxial material and FZ bulk enriched with oxygen, carbon, tin and platinum", Nucl. Phys. B (Proc. Suppl), vol.78, pp.645-649, 1999.

[4] A. Ruzin, G. Casse, M. Glaser, A. Zanet, F. Lemeilleur and S. Watts, "Comparison of radiation damage in silicon induced by protons and neutron irradiation", IEEE Trans. Nucl. Sci., vol.46, pp.1310-1313, 1999.

[5] G. Casse, P. P. Allport and M. Hanlon, "Improving the radiation hardness properties of silicon detectors using oxygenated n-type and p-type silicon", IEEE Trans. Nucl. Sci., vol.47, pp.527-532, 2000.

[6] M. Moll, E. Fretwurst and G. Lindstrom, "Leakage current of hadron irradiated silicon detectors - material dependence", Nucl. Instr. and Meth., vol.A 426, pp.87-93, 1999.

[7] D. Bisello, M. Descovich, A. Kaminsky, D. Pantano, J. Wyss and A. Zanet, “Radiation damage of oxygenated silicon diodes by 27 MeV protons", Il Nuovo Cimento, vol.A 112, pp.1377-1382, 1999.

[8] ROSE Collaboration, 3rd RD48 Status Report, CERN/LHCC 2000-009, 31 December 1999.

[9] J. Wyss, D. Bisello, A. Candelori, A. Kaminsky and D. Pantano, “Observation of an energy dependence of the radiation damage on standard and oxygenated silicon diodes by 16, 21, and 27 MeV protons”, Nucl. Instr. and Meth., vol.A, in press.

[10] "4th meeting on planning of work on oxygenated silicon detectors", RD48-ATLAS-CMS-LHCb, CERN, 15 June 2000.

[11] ITE, Institute of Electron Technology, Al. Lotnikow 32/46, 02-668, Warsaw, Poland.

[12] ST Microelectronics, Stradale Primosole 50, I-95121 Catania, Italy.

[13] ROSE Collaboration, Proposal, CERN/LHCC 96-23, P62/LHC R&D, 1996.

[14] Polovodice, Vovodvorska 994, 142-21 Prague 4, Czech Republic.

[15] ITME, Institute of Electronic Material Technology, ul. Wôlczinska 133, D1-919, Warsaw, Poland.

[16] Waker, AG, Burghausen, Germany.

[17] EVANS EUROPE, Brunel University, Uxbridge, Middlesex UB8 3PH, United Kingdom.

[18] J. Wyss, D. Bisello and D. Pantano, "SIRAD: an irradiation facility at the LNL Tandem accelerator for radiation damage studies on semiconductor detectors and electronic devices and systems”, Nucl. Instr. and Meth., vol.A, in press.

[19] SRIM-2000, Stopping and range of ions in matter, J. F. Zigler, IBM-Reasearch, Yorktown, NY, 10598, USA, http://www.research.ibm.com/ionbeams/.

[20] M. Hutinen and P. A. Aarnio, "Pion induced damage in silicon devices", Nucl. Instr. and Meth., vol.A 335, pp.580-582, 1993.

[21] A. Chilingarov, H. Feick, E. Fretwurst, G. Lindstrom, S. Roe and T. Schulz, "Radiation studies and operational projections for silicon in the ATLAS inner detector", Nucl. Instr. and Meth., vol.A 360, pp.432-437, 1995.